AIMS Mathematics, 11(8): 27508–27528.
DOI: 10.3934/math.20261101
Received: 05 July 2026
Revised: 20 August 2026
Accepted: 26 August 2026
Published: 31 August 2026

https://www.aimspress.com/journal/Math

Research article

Stability and bifurcation analysis in a commensalism model with saturation and efficiency constraints

Saad Jamhan Aldosari*

Department of Mathematics, College of Science and Humanities in Alkharj, Prince Sattam Bin Abdulaziz University, Alkharj 11942, Saudi Arabia

* **Correspondence:** Email: saad.aldosari@psau.edu.sa.

Abstract: Mathematical modeling of commensalism provides insights into ecological interactions in which one species benefits while the other remains unaffected. In this study, a discrete-time commensalism model is proposed by incorporating a saturating interaction benefit and an interaction efficiency parameter. In contrast to related models, the proposed formulation accounts for both the saturation of the commensal benefit and the fraction of the host population that is either ineffective or unavailable for interaction. The existence and stability of fixed points are analyzed, and conditions for period-doubling bifurcation are derived using the center manifold and normal form theories. Numerical simulations, including bifurcation diagrams, maximum Lyapunov exponents, phase portraits, and basins of attraction, confirm the theoretical results and reveal periodic, chaotic, and multistable dynamics. The findings demonstrate the important role of interaction efficiency and saturation in shaping commensal dynamics.

Keywords: population model; commensalism model; nonlinear dynamics; stability; bifurcation; chaos
Mathematics Subject Classification: 39A28, 39A30

1. Introduction

Mathematical modeling has a significant role to play in the understanding of interactions among various species in nature. This includes commensalism, a type of interaction in which one species benefits and the other is not affected. This is a one-sided advantage type of interaction. This type of interaction is frequently seen in nature. For example, epiphytic plants live on a tree to get sunlight, small fish live on a large animal for transport and food, or microorganisms live on a large animal to get nutrients. Similarly, cattle egrets follow cattle or buffaloes and feed on insects that are disturbed due to their movement, while the host remains unaffected. Moreover, there are insects found on tree

bark that feed on organic matter without harming the tree. All these interactions may look simple, but their effects on population dynamics may be complex. Such studies on simple interactions are useful in understanding species persistence, growth regulation, and ecological stability.

Over the last several decades, a number of mathematical models have been proposed for species interactions, including predator-prey systems [1, 2], competition systems [3, 4], amensalism systems [5, 6], and commensalism systems [7, 8]. Although predator-prey systems have been extensively studied, comparatively fewer studies have focused on the nonlinear dynamics and bifurcation behaviors of commensalism systems. However, several important contributions are available in the literature [7–10]. In general, classical commensalism systems assume that the beneficiary species enjoys a linear or unlimited advantage from the host species. However, this assumption is not valid in practical situations, as the advantage from the species interaction is limited due to environmental constraints.

Several studies have been conducted to reveal the dynamics of commensalism. In the study by Chen and Wu [11], the authors studied the commensal system of two species with a nonmonotonic functional response and showed that the system has a unique globally asymptotically stable positive equilibrium. In the study by Li and Wang [12], the authors studied the delayed commensalism model and showed that the model has a Hopf bifurcation and periodic oscillations in the presence of a time delay. In the study by He et al. [13], the authors incorporated the additive Allee effect into the Lotka Volterra commensal model and showed that the Allee effect has a great influence on the survival of the species and could cause the extinction of the species. Qu [14] studied a Beddington-DeAngelis type commensalism system with delays and investigated the existence of a Hopf bifurcation and persistence. Zhong et al. [15] studied a two-patch commensalism system with nonlinear dispersal and showed that dispersal and the Allee effect have a cooperative role in species persistence. Patra and Maitra [16] studied a three-species delayed commensalism system with control strategies and showed that the system is stable under appropriate control strategies.

To obtain a more realistic description of commensal interactions, it is necessary to include the phenomenon of saturation in the interaction term. This phenomenon of saturation implies that the benefit provided to the commensal species will not infinitely increase with the increase of the host population but will tend to a certain level. Furthermore, in nature, it is not uncommon to find inefficient interactions between species, in which not all individuals of the host species contribute in the same way to the benefit of the commensal species. This may occur because of spatial inactivity or inaccessibility. This phenomenon of partial interactions has not been considered in the commensalism models.

Inspired by the above observations, we introduce a commensalism model that includes the effects of saturation and the interaction efficiency parameter. The proposed continuous-time model is presented by the following:

$$\begin{cases} \dfrac{\mathrm{d}x}{\mathrm{d}t} = x\left(\alpha - \beta x + \frac{\gamma(1-r)y}{\eta+(1-r)y}\right), \\ \dfrac{\mathrm{d}y}{\mathrm{d}t} = y\left(\sigma - \tau y\right), \end{cases} \tag{1.1}$$

where $x(t)$ and $y(t)$ denote the population densities of the commensal (beneficiary) species and the host species, respectively. The parameter α represents the intrinsic growth rate of the commensal species, while β measures the strength of its intraspecific competition and therefore limits its growth at high population densities. The parameter γ denotes the maximum benefit that the commensal species can

obtain through its interaction with the host, whereas η is the half-saturation constant and determines how rapidly this interaction benefit approaches its maximum level.

A notable characteristic of this model is the parameter $r \in [0, 1)$, representing the proportion of the host species that is ineffective or unavailable for interaction. Therefore, only a proportion $(1 - r)y$ is available for growth of the commensal species. This represents a realistic ecological situation in which the interaction efficiency may be reduced for various reasons. The second equation represents the logistic growth for the host species, where σ is the intrinsic growth rate and τ represents intraspecific competition for the host species. Thus, the host follows logistic growth independent of the commensal population, which reflects the asymmetric nature of commensalism. Figure 1 presents a flowchart for system (1.1).

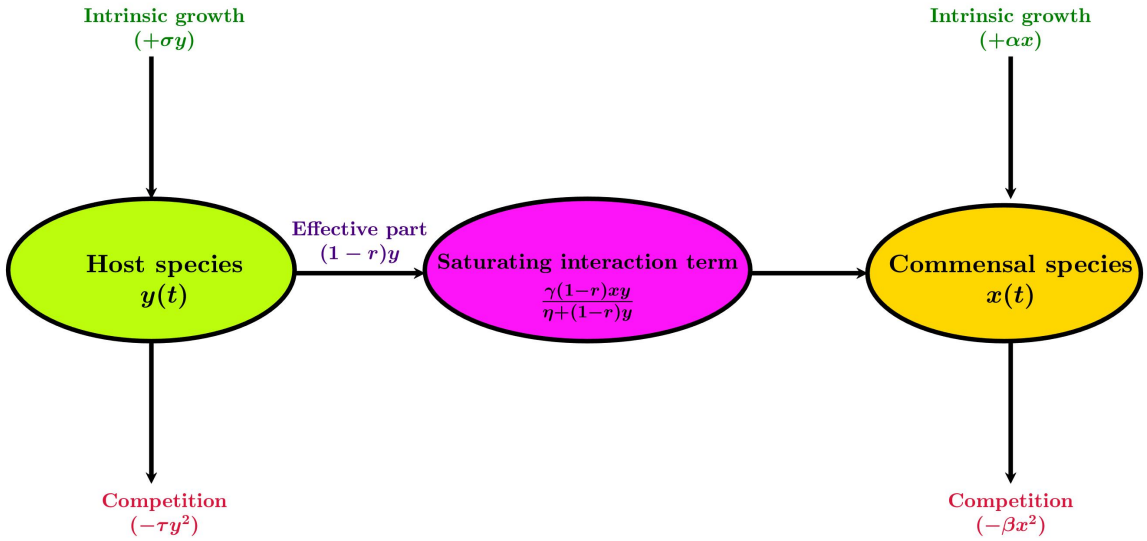

Figure 1. Schematic flowchart of system (1.1).

In [8], the authors considered a discrete model obtained from the following continuous-time system:

$$\begin{cases} \dfrac{\mathrm{d}x}{\mathrm{d}t} = x\left(\alpha - \beta x + \frac{\gamma y}{\eta + y^2}\right), \\ \dfrac{\mathrm{d}y}{\mathrm{d}t} = y\left(\sigma - \tau y\right). \end{cases} \tag{1.2}$$

The main difference between the model in [8] and the present model lies in the interaction term. In [8], the term $\frac{\gamma y}{\eta+y^2}$ first increases with y and then decreases when y becomes sufficiently large. In the present model, we use $\frac{\gamma(1-r)y}{\eta+(1-r)y}$, which increases with the effective interacting population $(1 - r)y$ and gradually approaches a saturation level. Here, $r \in [0, 1)$ represents the proportion of the second species that does not effectively participate in the interaction. Thus, the linear dependence on y in the denominator is used to describe a saturating commensal benefit, while the additional factor $1 - r$ allows us to account for the interaction efficiency.

The main novelty of the proposed model lies in incorporating both the saturation and interaction efficiencies into the commensal interaction. Unlike existing models, the interaction benefit depends

on the effective host population $(1 - r)y$, where $r \in [0, 1)$ represents the proportion of the host population that is ineffective or unavailable for interaction. Thus, the proposed model accounts not only for the saturation of the commensal benefit, but also for the fact that not all individuals of the host population equally contribute to the interaction. This formulation provides a distinct framework to investigate how the interaction efficiency influences the stability and complex dynamics of a discrete commensalism system.

Although the host equation independently evolves and has a logistic form, the proposed system (1.1) is triangular rather than fully decoupled, since the dynamics of the commensal population depend nonlinearly on the host population through the saturating term $\frac{\gamma(1-r)y}{\eta+(1-r)y}$. Consequently, the long-term behavior of the commensal population is governed by the combined effects of the host dynamics, saturation, and interaction efficiency.

While continuous time models have their advantages, some ecological processes occur in discrete time, such as seasonal reproduction and generational turnover. Moreover, discrete time models have richer dynamics, including period doubling cascades and chaos [17–19], which are not possible in two-dimensional continuous autonomous systems due to the Poincare Bendixson theorem [20]. Hence, it is of interest to consider the discrete version of system (1.1). Moreover, various numerical and discretization techniques have been developed for nonlinear biological models to obtain reliable discrete approximations and preserve important qualitative properties of the underlying systems [21–24].

Using the forward Euler method [25, 26], we obtain the following discrete model:

$$\begin{cases} x_{n+1} = x_n + hx_n\left(\alpha - \beta x_n + \frac{\gamma(1-r)y_n}{\eta+(1-r)y_n}\right), \\ y_{n+1} = y_n + hy_n\left(\sigma - \tau y_n\right), \end{cases} \tag{1.3}$$

where $h > 0$ is the step size. This discrete formulation enables us to explore how parameter variations and discretization affect the system stability and bifurcation behavior.

The main aim of this research is to examine the dynamical behavior of the proposed discrete commensalism model. Specifically, we examine the existence and stability of equilibrium points and the existence of a bifurcation, especially a period doubling bifurcation, which is a primary mechanism of chaos. The introduction of the interaction efficiency parameter r sheds light on the effect of partial interaction.

The rest of the paper is outlined as follows: In Section 2, the existence and stability analyses of equilibrium points are discussed; in Section 3, a bifurcation analysis is presented; numerical examples are given in Section 4; and conclusions are drawn in Section 5.

2. Stability analysis of fixed points

It is vital to understand the stability of fixed points, especially when dealing with commensalism systems, where fixed points are considered to be equilibrium points where the populations of both species are constant over time. By understanding the stability of fixed points, it is possible to forecast the behavior of the system over time, especially with regard to the survival of the commensal species. From a biological perspective, fixed points can be considered to be the steady state of the ecosystem, where their stability is vital in understanding the effects of the interaction.

The fixed points (x, y) for system (1.3) can be obtained by solving the following system:

$$\begin{cases} x = x + hx\Big(\alpha - \beta x + \frac{\gamma(1-r)y}{\eta+(1-r)y}\Big), \\ y = y + hy\Big(\sigma - \tau y\Big). \end{cases} \tag{2.1}$$

The discrete system (1.3) admits four fixed points given by the following:

$$E_0 = (0, 0),\ E_1 = \left(\frac{\alpha}{\beta}, 0\right),\ E_2 = \left(0, \frac{\sigma}{\tau}\right),\ E^* = \left(\frac{\alpha + \frac{(1-r)\gamma\sigma}{(1-r)\sigma+\eta\tau}}{\beta}, \frac{\sigma}{\tau}\right).$$

Each of these fixed points has a clear ecological interpretation:

- $E_0 = (0, 0)$ is the extinction equilibrium, where both the commensal species and the host species are absent from the system.
- $E_1 = \left(\frac{\alpha}{\beta}, 0\right)$ is the survival equilibrium of the commensal species without the host species. In this equilibrium, the commensal species is present, with its population size at its carrying capacity, driven by its intrinsic growth rate and intraspecies competition.
- $E_2 = \left(0, \frac{\sigma}{\tau}\right)$ is the equilibrium where only the host species is present, driven by logistic growth, while the commensal species becomes extinct.
- E^* is the equilibrium where both species coexist, with the commensal species benefiting from the presence of the host species due to the saturating effect, while the host species is unaffected by the commensal species, reflecting the asymmetric nature of commensalism.

The Jacobian matrix of the model

$$\begin{cases} x_{n+1} = f(x_n, y_n), \\ y_{n+1} = g(x_n, y_n) \end{cases}$$

is the matrix given below:

$$J(x, y) = \begin{bmatrix} \frac{\partial f}{\partial x} & \frac{\partial f}{\partial y} \\ \frac{\partial g}{\partial x} & \frac{\partial g}{\partial y} \end{bmatrix}.$$

In order to classify the fixed points, we follow the method described in [27, 28]. The Jacobian matrix $J(x, y)$ of model (1.3) evaluated at any point (x, y) is as follows:

$$J(x, y) = \begin{bmatrix} 1 + h\left(\alpha - 2x\beta - \frac{(-1+r)y\gamma}{y-ry+\eta}\right) & -\frac{h(-1+r)xy\eta}{(y-ry+\eta)^2} \\ 0 & 1 + h(\sigma - 2y\tau) \end{bmatrix}.$$

Proposition 2.1. *The trivial fixed point E_0 is always a source.*

Proof. We obtain the following:

$$J(E_0) = \begin{bmatrix} 1 + h\alpha & 0 \\ 0 & 1 + h\sigma \end{bmatrix}.$$

The eigenvalues of $J(E_0)$ are given by $\xi_1 = 1 + h\alpha$ and $\xi_2 = 1 + h\sigma$. It is evident that both eigenvalues satisfy $\xi_{1,2} > 1$. Hence, the equilibrium point E_0 is unstable and behaves as a source. □

Proposition 2.2. *E_1 is*

1. *never a sink,*
2. *a source if $h > \frac{2}{\alpha}$,*
3. *a saddle if $h < \frac{2}{\alpha}$,*
4. *nonhyperbolic and* (1.3) *goes through period-doubling bifurcation at E_1 when $h = \frac{2}{\alpha}$.*

Proof. We obtain the following:

$$J(E_1) = \begin{bmatrix} 1 - h\alpha & -\frac{h(-1+r)\alpha\gamma}{\beta\eta} \\ 0 & 1 + h\sigma \end{bmatrix}.$$

The eigenvalues of $J(E_1)$ are $\xi_1 = 1 - h\alpha$ and $\xi_2 = 1 + h\sigma$. It is clear that $\xi_2 > 1$. Moreover,

$$|\xi_1| \begin{cases} < 1, & \text{if } h < \frac{2}{\alpha}, \\ = 1, & \text{if } h = \frac{2}{\alpha}, \\ > 1, & \text{if } h > \frac{2}{\alpha}. \end{cases} \tag{2.2}$$

□

Proposition 2.3. *E_2 is*

1. *never a sink,*
2. *a source if $h > \frac{2}{\sigma}$,*
3. *a saddle if $h < \frac{2}{\sigma}$,*
4. *nonhyperbolic and* (1.3) *undergoes period-doubling bifurcation at E_2 when $h = \frac{2}{\sigma}$.*

Proof. We obtain the following:

$$J(E_2) = \begin{bmatrix} 1 + h\left(\alpha + \frac{(1-r)\gamma\sigma}{(1-r)\sigma+\eta\tau}\right) & 0 \\ 0 & 1 - h\sigma \end{bmatrix}.$$

The eigenvalues of $J(E_2)$ are given by $\xi_1 = 1 + h\left(\alpha + \frac{(1-r)\gamma\sigma}{(1-r)\sigma+\eta\tau}\right)$ and $\xi_2 = 1 - h\sigma$. It is evident that $\xi_1 > 1$. Moreover,

$$|\xi_2| \begin{cases} < 1, & \text{if } h < \frac{2}{\sigma}, \\ = 1, & \text{if } h = \frac{2}{\sigma}, \\ > 1, & \text{if } h > \frac{2}{\sigma}. \end{cases} \tag{2.3}$$

□

Proposition 2.4. *E^* is*

1. *a sink if $h < \min\left\{\frac{2}{\sigma}, \frac{-2\eta\tau+2r\sigma-2\sigma}{-\alpha\eta\tau-\alpha\sigma-\gamma\sigma+\alpha r\sigma+\gamma r\sigma}\right\}$,*

2. *a source if* $h > \max\left\{\frac{2}{\sigma}, \frac{-2\eta\tau+2r\sigma-2\sigma}{-\alpha\eta\tau-\alpha\sigma-\gamma\sigma+\alpha r\sigma+\gamma r\sigma}\right\}$,

3. *a saddle if one of the subsequent conditions is fulfilled:*

   (i) $\frac{2}{\sigma} < h < \frac{-2\eta\tau+2r\sigma-2\sigma}{-\alpha\eta\tau-\alpha\sigma-\gamma\sigma+\alpha r\sigma+\gamma r\sigma}$,

   (ii) $\frac{-2\eta\tau+2r\sigma-2\sigma}{-\alpha\eta\tau-\alpha\sigma-\gamma\sigma+\alpha r\sigma+\gamma r\sigma} < h < \frac{2}{\sigma}$,

4. *nonhyperbolic and* (1.3) *goes through period-doubling bifurcation at* E^* *when either of the subsequent requirements is met:*

   (i) $h = \frac{2}{\sigma}$,

   (ii) $h = \frac{-2\eta\tau+2r\sigma-2\sigma}{-\alpha\eta\tau-\alpha\sigma-\gamma\sigma+\alpha r\sigma+\gamma r\sigma}$.

Proof. We obtain the following:

$$J(E^*) = \begin{bmatrix} 1 - h\alpha + \frac{h(-1+r)\gamma\sigma}{\sigma-r\sigma+\eta\tau} & -\frac{h(-1+r)\gamma\eta\tau^2(-((-1+r)(\alpha+\gamma)\sigma)+\alpha\eta\tau)}{\beta(\sigma-r\sigma+\eta\tau)^3} \\ 0 & 1 - h\sigma \end{bmatrix}. \tag{2.4}$$

The eigenvalues of $J(E^*)$ are $\xi_1 = 1 - h\alpha + \frac{h(-1+r)\gamma\sigma}{\sigma-r\sigma+\eta\tau}$ and $\xi_2 = 1 - h\sigma$. It follows that

$$|\xi_1| \begin{cases} < 1, & \text{if } h < \frac{-2\eta\tau+2r\sigma-2\sigma}{-\alpha\eta\tau-\alpha\sigma-\gamma\sigma+\alpha r\sigma+\gamma r\sigma}, \\ = 1, & \text{if } h = \frac{-2\eta\tau+2r\sigma-2\sigma}{-\alpha\eta\tau-\alpha\sigma-\gamma\sigma+\alpha r\sigma+\gamma r\sigma}, \\ > 1, & \text{if } h > \frac{-2\eta\tau+2r\sigma-2\sigma}{-\alpha\eta\tau-\alpha\sigma-\gamma\sigma+\alpha r\sigma+\gamma r\sigma}. \end{cases} \tag{2.5}$$

Moreover,

$$|\xi_2| \begin{cases} < 1, & \text{if } h < \frac{2}{\sigma}, \\ = 1, & \text{if } h = \frac{2}{\sigma}, \\ > 1, & \text{if } h > \frac{2}{\sigma}. \end{cases} \tag{2.6}$$

□

3. Bifurcation analysis

In this section, we look into the bifurcation behavior of the proposed system, thereby focusing on a period-doubling bifurcation at E^*. By changing h, we examine how the stability of the equilibrium shifts and identify the conditions that lead the system from a stable behavior to periodic dynamics. This analysis helps explain the development of complex dynamics in the commensalism model. For a better understanding of the bifurcation analysis, we refer readers to the references [29–31].

We examine the period doubling bifurcation at point E^* based on Condition 4(*ii*) as described in Proposition 2.4. The analysis proceeds through several standard steps. First, the bifurcation parameter is perturbed near its critical value, and the coexistence equilibrium is shifted to the origin. Next, a linear transformation is introduced to diagonalize the linear part of the system and isolate the

critical eigendirection. Then, the center manifold theorem is applied to reduce the dynamics to a one-dimensional map on the center manifold. Finally, the normal form theory is used to derive the bifurcation conditions and determine the stability of the bifurcating period-2 orbit.

A small perturbation ϵ in h around $h_1 = \frac{-2\eta\tau+2r\sigma-2\sigma}{-\alpha\eta\tau-\alpha\sigma-\gamma\sigma+\alpha r\sigma+\gamma r\sigma}$ in system (1.3) leads to the following:

$$\begin{cases} x_{n+1} = x_n + (h_1+\epsilon)x_n\Big(\alpha - \beta x_n + \frac{\gamma(1-r)y_n}{\eta+(1-r)y_n}\Big), \\ y_{n+1} = y_n + (h_1+\epsilon)y_n\Big(\sigma - \tau y_n\Big). \end{cases} \tag{3.1}$$

To shift E^* to $(0,0)$, we introduce the following change of variables:

$$\lambda_n = x_n - \frac{\alpha + \frac{(1-r)\gamma\sigma}{(1-r)\sigma+\eta\tau}}{\beta}, \qquad \rho_n = y_n - \frac{\sigma}{\tau}.$$

Consequently, system (3.1) can be rewritten in the following form:

$$\begin{bmatrix} \lambda_{n+1} \\ \rho_{n+1} \end{bmatrix} = \begin{bmatrix} -1 & -\frac{2(-1+r)\gamma\eta\tau^2}{\beta(\sigma-r\sigma+\eta\tau)^2} \\ 0 & 1 - \frac{2\sigma((-1+r)\sigma-\eta\tau)}{(-1+r)\alpha\sigma+(-1+r)\gamma\sigma-\alpha\eta\tau} \end{bmatrix} \begin{bmatrix} \lambda_n \\ \rho_n \end{bmatrix} + \begin{bmatrix} \mathbb{F}_1(\lambda_n,\rho_n,\epsilon) \\ \mathbb{F}_2(\lambda_n,\rho_n,\epsilon) \end{bmatrix}, \tag{3.2}$$

where

$$\mathbb{F}_1(\lambda_n,\rho_n,\epsilon) = a_1\lambda_n^2 + a_2\rho_n^2 + a_3\lambda_n\rho_n + a_4\lambda_n\epsilon + a_5\rho_n\epsilon + a_6\rho_n^3 + a_7\lambda_n^2\epsilon + a_8\lambda_n\rho_n^2 + a_9\rho_n^2\epsilon + a_{10}\lambda_n\rho_n\epsilon + O(4),$$
$$\mathbb{F}_2(\lambda_n,\rho_n,\epsilon) = b_1\rho_n^2 + b_2\rho_n\epsilon + b_3\rho_n^2\epsilon.$$

The nonlinear functions $\mathbb{F}_1$ and $\mathbb{F}_2$ are obtained by expanding the transformed system (3.1) about $(\lambda_n,\rho_n,\epsilon) = (0,0,0)$ and retaining terms up to third order. Therefore, the coefficients a_i and b_j are the corresponding coefficients of the quadratic and cubic terms in this Taylor expansion. Since their explicit expressions are lengthy, they are provided in Appendix A. Next, we introduce a linear transformation that converts the linear part of system (3.2) into a diagonal form. This transformation decouples the directions corresponding to the eigenvalues of the Jacobian matrix, allowing the critical mode associated with the eigenvalue -1 to be isolated from the stable mode. As a result, the center manifold reduction and the derivation of the normal form become considerably simpler. system (3.2) is diagonalized by applying the following transformation:

$$\begin{bmatrix} \lambda_n \\ \rho_n \end{bmatrix} = \begin{bmatrix} 1 & -\frac{(-1+r)\gamma\eta\tau^2(-\alpha\sigma+r\alpha\sigma-\gamma\sigma+r\gamma\sigma-\alpha\eta\tau)}{\beta(\sigma-r\sigma+\eta\tau)^2\left(-\alpha\sigma+r\alpha\sigma-\gamma\sigma+r\gamma\sigma+\sigma^2-r\sigma^2-\alpha\eta\tau+\eta\sigma\tau\right)} \\ 0 & 1 \end{bmatrix} \begin{bmatrix} \kappa_n \\ \theta_n \end{bmatrix}. \tag{3.3}$$

Under the transformation (3.3), (3.2) is transformed to the following:

$$\begin{bmatrix} \kappa_{n+1} \\ \theta_{n+1} \end{bmatrix} = \begin{bmatrix} -1 & 0 \\ 0 & 1 + \frac{2\sigma(\sigma-r\sigma+\eta\tau)}{(-1+r)(\alpha+\gamma)\sigma-\alpha\eta\tau} \end{bmatrix} \begin{bmatrix} \kappa_n \\ \theta_n \end{bmatrix} + \begin{bmatrix} \mathbb{G}_1(\kappa_n,\theta_n,\epsilon) \\ \mathbb{G}_2(\kappa_n,\theta_n,\epsilon) \end{bmatrix}, \tag{3.4}$$

where

$$\mathbb{G}_1(\kappa_n,\theta_n,\epsilon) = c_1\kappa_n^2 + c_2\theta_n^2 + c_3\kappa_n\theta_n + c_4\kappa_n\epsilon + c_5\theta_n^3 + c_6\kappa_n^2\epsilon + c_7\kappa_n\theta_n^2 + c_8\theta_n^2\epsilon + c_9\kappa_n\theta_n\epsilon + O(4),$$

$$\mathbb{G}_2(\kappa_n, \theta_n, \epsilon) = d_1\theta_n^2 + d_2\theta_n\epsilon + d_3\theta_n^2\epsilon.$$

The coefficients c_i and d_j are listed in Appendix B. Next, let Q^C be the center manifold of (3.4) at the origin in a small neighborhood of $\epsilon = 0$. It can be computed in the following form:

$$Q^C = \left\{(\kappa_n, \theta_n, \epsilon) \in \mathbb{R}^3_+ \middle| \theta_n = p_1\kappa_n^2 + p_2\kappa_n\epsilon + p_3\epsilon^2 + O(3)\right\}.$$

Substituting the center-manifold representation into the invariance equation associated with (3.4) and comparing the coefficients of κ_n^2, $\kappa_n\epsilon$, and ϵ^2 on both sides gives $p_1 = p_2 = p_3 = 0$. Consequently, the restriction of (3.4) to the center manifold yields the following:

$$\tilde{F} := \kappa_{n+1} = -\kappa_n + \left(\frac{2\beta(\sigma - r\sigma + \eta\tau)}{(-1+r)(\alpha+\gamma)\sigma - \alpha\eta\tau}\right)\kappa_n^2 + \left(-\alpha + \frac{(-1+r)\gamma\sigma}{\sigma - r\sigma + \eta\tau}\right)\kappa_n\epsilon - \beta\kappa_n^2\epsilon + O(4). \tag{3.5}$$

To verify the nondegeneracy conditions for a period-doubling bifurcation, we compute the normal-form coefficients l_1 and l_2. The condition $l_1 \neq 0$ ensures that the critical eigenvalue crosses -1 nondegenerately as the bifurcation parameter h passes through h_1, whereas $l_2 \neq 0$ guarantees that the leading nonlinear term responsible for the creation of the period-2 orbit does not vanish. These coefficients are given by the following:

$$l_1 = \tilde{F}_\epsilon\tilde{F}_{\kappa_n\kappa_n} + 2\tilde{F}_{\kappa_n\epsilon}\Big|_{(0,0)} = \frac{2((1-r)\gamma\sigma + \alpha(\sigma - r\sigma + \eta\tau))}{(-1+r)\sigma - \eta\tau}, \tag{3.6}$$

$$l_2 = \frac{1}{2}(\tilde{F}_{\kappa_n\kappa_n})^2 + \frac{1}{3}\tilde{F}_{\kappa_n\kappa_n\kappa_n}\Big|_{(0,0)} = \frac{8\beta^2(\sigma - r\sigma + \eta\tau)^2}{((-1+r)\alpha\sigma + (-1+r)\gamma\sigma - \alpha\eta\tau)^2}. \tag{3.7}$$

Under the assumed parameter conditions, $l_1 < 0$ and $l_2 > 0$, and hence, both nondegeneracy conditions are satisfied. The nonzero value of l_1 confirms the transversal passage of the critical multiplier through -1, while $l_2 > 0$ determines the emergence of a stable period-2 orbit from E^*. Hence, we obtain the following result.

Theorem 3.1. *Suppose that Condition* 4(*ii*) *of Proposition 2.4 is true. Then,* (1.3) *undergoes a period-doubling bifurcation at E^* as h varies through $h_1 = \frac{-2\eta\tau+2r\sigma-2\sigma}{-\alpha\eta\tau-\alpha\sigma-\gamma\sigma+\alpha r\sigma+\gamma r\sigma}$. Additionally, since $l_2 > 0$, a stable period-2 orbit of system* (1.3) *emerges from E^*.*

4. Numerical examples

In this section, some numerical simulations are presented to verify the theoretical results and to demonstrate the complex dynamics of system (1.3). The parameter sets used in the numerical simulations are hypothetically selected to satisfy the analytically derived stability and bifurcation conditions and to illustrate the different dynamical regimes of the model.

All numerical simulations are carried out in MATLAB R2023a. In constructing the bifurcation diagrams, the selected bifurcation parameter is varied across the specified interval using 1500 uniformly distributed sample points. For each sampled parameter value, system (1.3) is simulated for a total of $N = 8000$ iterations starting from the prescribed initial condition. The initial 6500 iterations are omitted to remove transient dynamics, while the remaining 1500 iterates are retained to plot the bifurcation structure. The phase-plane trajectories are produced with the same initial

conditions and simulation horizon after excluding the first 300 iterations as transient behavior. The maximum Lyapunov exponent (MLE) is evaluated through the conventional Jacobian-based tangent vector approach, where the perturbation vector is normalized at each iteration to maintain numerical stability. In this computation, the first 800 iterations are disregarded as transients, and the MLE is subsequently approximated using the following 1000 iterations.

4.1. Parameter sensitivity

A sensitivity analysis is a useful technique for mathematical modeling, and it helps us quantify how changes in the parameters of a system affect the results. It is a useful technique for systems where the overall stability of the system is controlled by several parameters. Some of the fields where this technique is useful include economics, ecology, and engineering. The sensitivity index related to a parameter p is defined as follows:

$$S_p = \frac{\partial x^*}{\partial p} \times \frac{p}{x^*},$$

where x^* represents the equilibrium value of the system. A positive sensitivity index implies that the parameter has a magnifying effect on the system's equilibrium population, whereas a negative value implies a suppressing effect. A sensitivity index close to zero implies that the parameter has little or no effect on the system.

The sensitivity indices for the commensal population, as presented in Figure 2 for different parameter sets, show that β has a significant negative effect on the equilibrium, thereby showing that intraspecific competition is an important factor, thus causing the population to decrease. On the other hand, the effect of α is positive, thereby showing that it favors the growth of the population. The effect of the interaction parameter γ is positive, while η and r have negative effects due to saturation and an ineffective host proportion, respectively. The parameters σ and τ have an indirect effect on the commensal population, thereby showing moderate effects.

For the host population, the equilibrium is $y^* = \frac{\sigma}{\tau}$, and thus, the sensitivity indices for this population remain constant for all cases with $S_\sigma = 1$ and $S_\tau = -1$, whereas the remaining parameters have no influence. This suggests that the dynamics of the host are only driven by its intrinsic growth and self-limitation, whereas the commensal population is driven by both intrinsic and interaction parameters. Overall, Figure 2 indicates that the commensal population is most strongly affected by its intraspecific competition, while the interaction-related parameters modify its equilibrium level to different degrees.

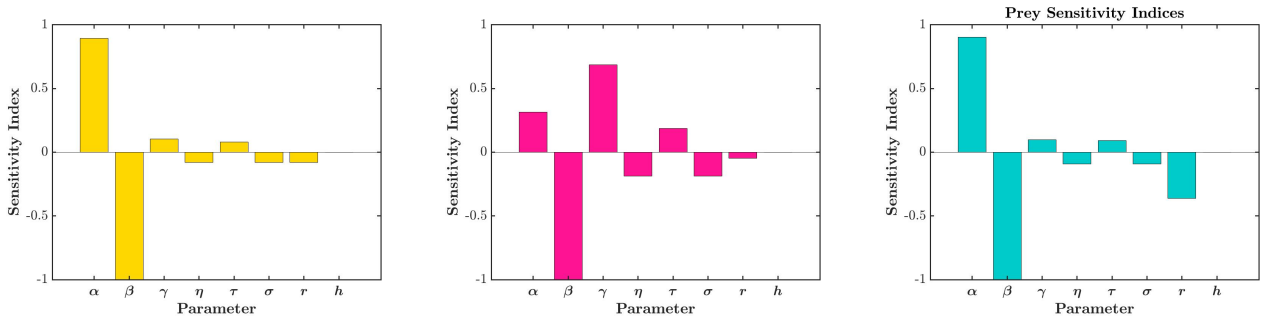

Figure 2. Sensitivity analysis of the model with respect to the beneficiary species x_n is carried out for three distinct parameter sets. These three cases correspond to the following parameter configurations: (a) $\alpha = 1.8, \beta = 1.1, \gamma = 0.9, \eta = 0.7, \tau = 1.4, \sigma = 0.6, r = 0.5$, and $h = 0.98$, (b) $\alpha = 0.6, \beta = 1.2, \gamma = 1.8, \eta = 0.3, \tau = 1, \sigma = 1, r = 0.2$, and $h = 0.98$, (c) $\alpha = 1, \beta = 1.1, \gamma = 1.5, \eta = 1.4, \tau = 2.2, \sigma = 1.2, r = 0.8$, and $h = 0.98$.

4.2. Bifurcation analysis varying h

To explore the dynamic behavior of system (1.3), the role of the step size h is analyzed, which is very important in discrete models and might affect the stability of the system. From the biological point of view, h is viewed as a time scaling factor to update the population system, and a larger h might cause instability in the system.

The parameter values used in this example are $\alpha = 1.8, \beta = 1.1, \gamma = 0.9, \eta = 0.7, \sigma = 0.6, \tau = 1.4$, and $r = 0.5$. Under this set of parameters, a period-doubling bifurcation occurs at $h_1 = 0.994561$. The coexistence fixed point is $E^* = (1.82813, 0.428571)$. At this fixed point, eigenvalues of $J(E^*)$ are $\xi_1 = -1$ and $\xi_2 = 0.403263$. This again proves the occurrence of a period-doubling bifurcation in accordance with Theorem 3.1. In addition, the calculated coefficients $l_1 = -4.02188 \neq 0$ and $l_2 = 2.39375 \neq 0$ satisfy the required theoretical conditions. Since $l_2 > 0$, a stable period-2 orbit bifurcates from the equilibrium E^*.

The bifurcation diagram for x_n with respect to h over the range $[0.8, 1.5]$ is shown in Figure 3(a). This diagram clearly shows the route to chaos from stability by means of period-doubling bifurcations. The MLE corresponding to the above is shown in Figure 3(b). The negative values correspond to a stable or periodic behavior, while the positive values verify the chaotic behavior.

Further information about the system behavior can be found by analyzing the time series and phase portraits presented in Figure 4. For $h = 0.99$, the system tends to the stable equilibrium E^*. For $h = 1.1$, the system has a stable period-2 cycle, followed by period-4 and period-8 cycles at $h = 1.25$ and $h = 1.27$, respectively. This is the classical period-doubling route to chaos. For slightly larger values of h, namely $h = 1.28$ and $h = 1.33$, the system shows irregular behaviors, thus verifying the chaotic behavior. It is interesting to note that at $h = 1.41$, the system shows a period-3 cycle. It is well known that if a period-3 cycle exists, then the system is chaotic. This is further verified by the chaotic behavior at $h = 1.45$.

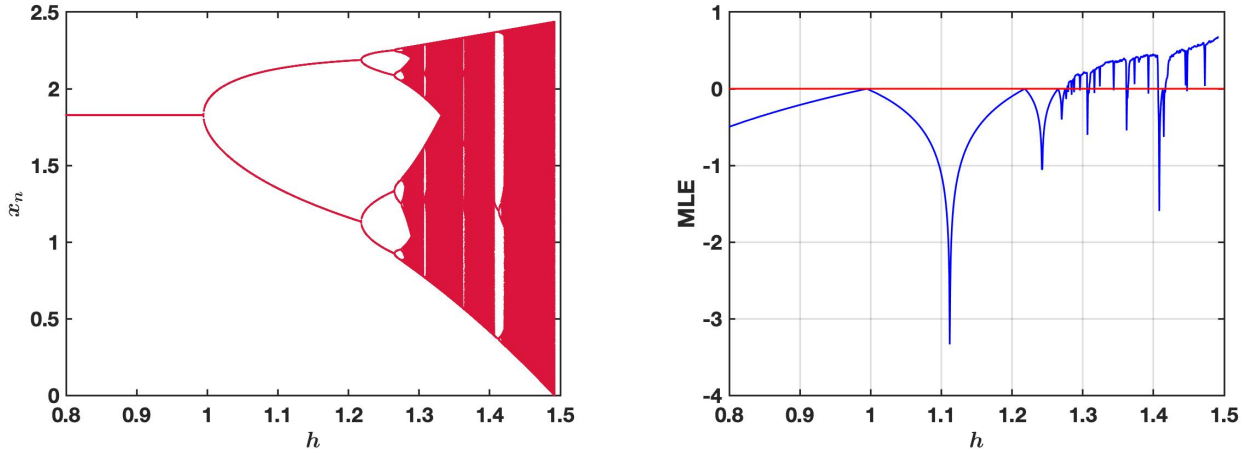

(a) **(b)**

Figure 3. Bifurcation diagram of x_n and MLE plot for (1.3) varying h and fixing $\alpha = 1.8, \beta = 1.1, \gamma = 0.9, \eta = 0.7, \sigma = 0.6, \tau = 1.4$, and $r = 0.5$, and the initial conditions are $x_0 = 1.8, y_0 = 0.4$.

From an ecological point of view, the results here show that increasing the time-step parameter h can cause instability in the coexistence equilibrium, thus resulting in oscillations and chaotic fluctuations in population densities. This indicates that discrete effects, such as seasonal reproduction, play a critical role in the dynamics of commensal systems.

Figure 5 illustrates the basins of attraction for five different parameter sets given in Table 1. The plots demonstrate that the long-term dynamics strongly depend on the initial conditions, with multiple attractors coexisting for the same parameter values. The basin boundaries are highly intricate and interwoven, thus indicating a pronounced sensitivity to the initial conditions. Consequently, even small perturbations in the initial population densities can drive the system toward qualitatively different asymptotic behaviors, thus confirming the presence of multistability.

More specifically, Figure 5(a) shows the coexistence of a period-4 orbit and a chaotic attractor. Figure 5(b) illustrates the coexistence of a period-2 orbit and a chaotic attractor. Figure 5(c) presents the basins of attraction corresponding to period-2 and period-6 orbits. Figure 5(d) depicts the coexistence of period-2 and period-12 orbits, while Figure 5(e) shows the coexistence of a period-8 orbit and a chaotic attractor. These highlight the rich multistable behavior of the proposed system.

An important implication of Figure 5 is that the parameter values alone may not uniquely determine the long-term population behavior. For the same ecological conditions, different initial population densities can lead to periodic or chaotic states. Therefore, the initial abundance of the two species can play an important role in determining the eventual dynamical regime of the system.

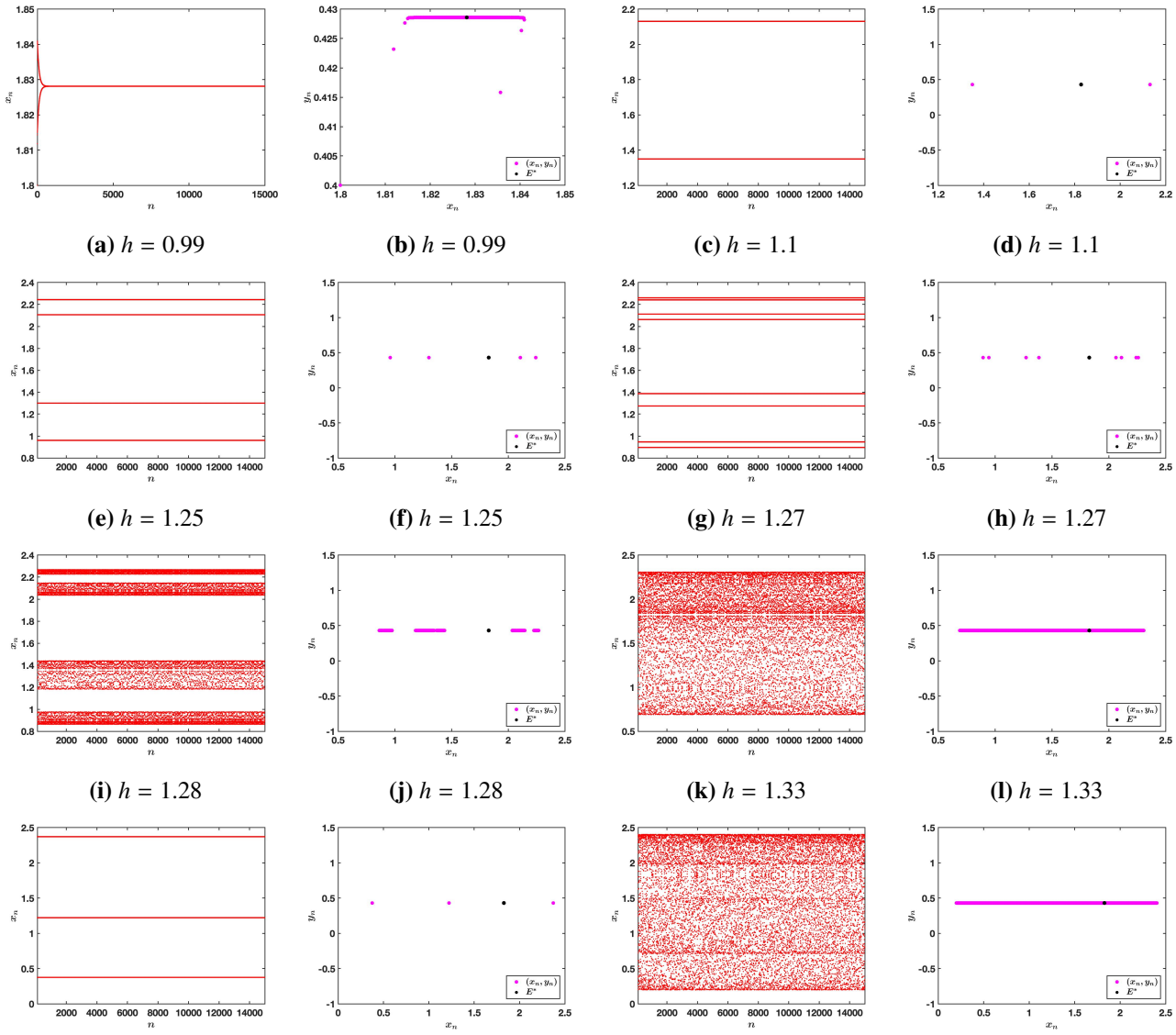

(a) $h = 0.99$ **(b)** $h = 0.99$ **(c)** $h = 1.1$ **(d)** $h = 1.1$

(e) $h = 1.25$ **(f)** $h = 1.25$ **(g)** $h = 1.27$ **(h)** $h = 1.27$

(i) $h = 1.28$ **(j)** $h = 1.28$ **(k)** $h = 1.33$ **(l)** $h = 1.33$

(m) $h = 1.41$ **(n)** $h = 1.41$ **(o)** $h = 1.45$ **(p)** $h = 1.45$

Figure 4. Phase diagrams of (1.3) for different values of h by setting $\alpha = 1.8, \beta = 1.1, \gamma = 0.9, \eta = 0.7, \sigma = 0.6, \tau = 1.4, r = 0.5, x_0 = 1.8$, and $y_0 = 0.4$.

Table 1. Parameter values used for the basin of attraction plots.

Figure	Parameter values
Figure 5(a)	$\alpha = 1.751922,\ \beta = 0.536604,\ \gamma = 0.235217,\ \eta = 1.358819,$ $\sigma = 1.480789,\ \tau = 0.890885,\ r = 0.610368,\ h = 1.407425.$
Figure 5(b)	$\alpha = 0.957929,\ \beta = 1.570816,\ \gamma = 0.821931,\ \eta = 1.411217,$ $\sigma = 0.878731,\ \tau = 1.150870,\ r = 0.632917,\ h = 2.333950.$
Figure 5(c)	$\alpha = 0.995630,\ \beta = 2.297181,\ \gamma = 0.598378,\ \eta = 1.052267,$ $\sigma = 1.013250,\ \tau = 1.786230,\ r = 0.573994,\ h = 2.251798.$
Figure 5(d)	$\alpha = 1.399027,\ \beta = 0.518909,\ \gamma = 0.262037,\ \eta = 1.465992,$ $\sigma = 1.365260,\ \tau = 1.137360,\ r = 0.420068,\ h = 1.725503.$
Figure 5(e)	$\alpha = 1.65,\ \beta = 0.62,\ \gamma = 0.35,\ \eta = 1.25,\ \sigma = 1.42,\ \tau = 0.95,$ $r = 0.58,\ h = 1.48.$

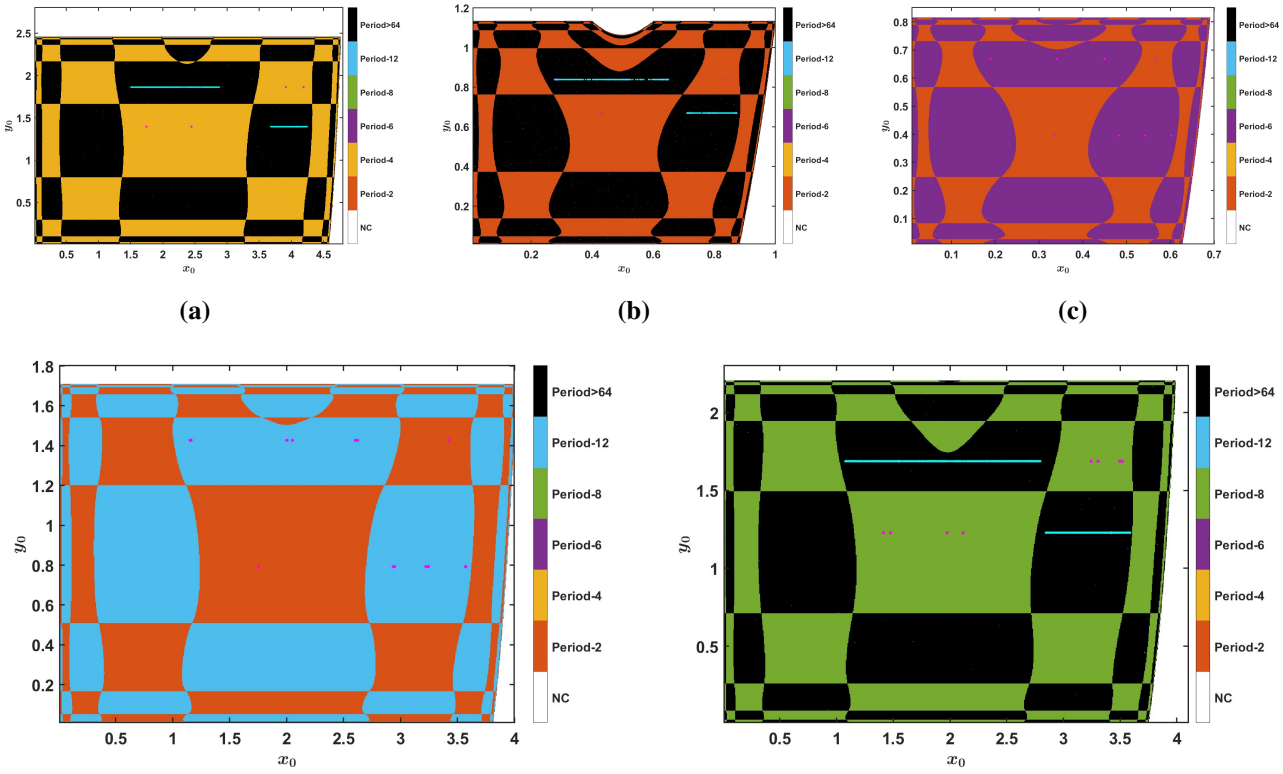

Figure 5. Basin of attraction plots showing multistability.

4.3. Bifurcation analysis with respect to r and its ecological influence

Now, let us examine the influence of the interaction efficiency parameter r on the dynamics of system (1.3). Recall that the proportion of the host population that is ineffective or unavailable for interaction is represented by the interaction efficiency parameter $r \in [0, 1)$, and this plays a vital role in governing the commensal benefit.

We assume that $\alpha = 1.8, \beta = 1.1, \gamma = 0.9, \eta = 0.7, \sigma = 0.6, \tau = 1.4$, and $h = 1$. In this case, the period-doubling bifurcation occurs when $r = 0.533333$, and the coexisting equilibrium is given by $E^* = (1.81818, 0.428571)$. The eigenvalues of $J(E^*)$ are $\xi_1 = -1$ and $\xi_2 = 0.4$, which verifies the occurrence of a period-doubling bifurcation as stated in Theorem 3.1.

In Figure 6(a), we plotted the bifurcation diagram of x_n when the parameter r is varied in the range $[0.01, 0.85]$. The MLE of the system is plotted in Figure 6(b). The results clearly show that the system loses stability for smaller values of r, and this instability is due to a period-doubling bifurcation. For larger values of r, the coexistence equilibrium point E^* is stable, and this shows that the system becomes stable as the parameter r increases.

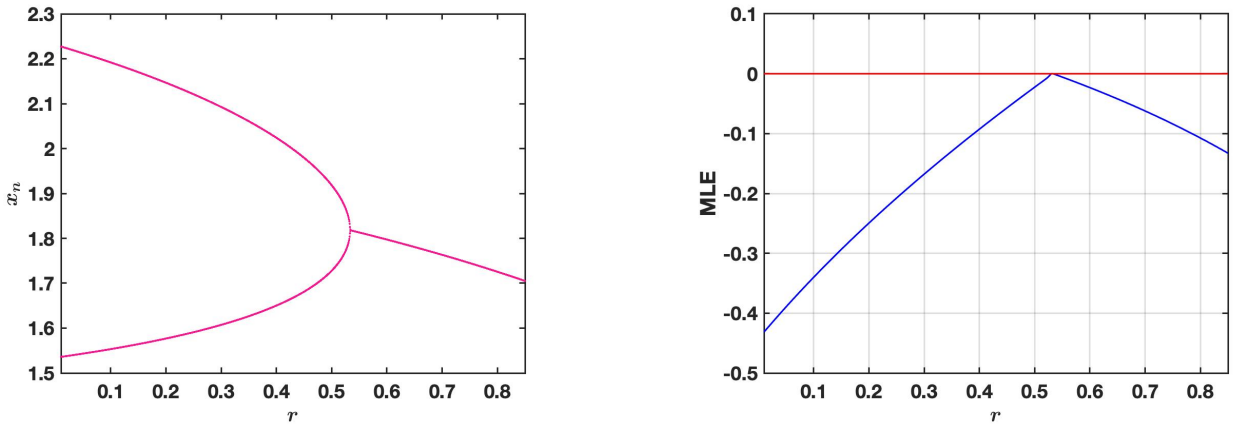

(a) **(b)**

Figure 6. Bifurcation diagrams and MLE plot of (1.3) varying r and fixing $\alpha = 1.8, \beta = 1.1, \gamma = 0.9, \eta = 0.7, \sigma = 0.6, \tau = 1.4$, and $h = 1$, and the initial conditions are $x_0 = 1.8, y_0 = 0.4$.

From an ecological perspective, this behavior can be explained by the fact that larger values of r reduce the effective interaction between the species, thereby weakening the nonlinear feedback that drives the complex dynamics. Consequently, reducing the effective commensal benefit suppresses periodic fluctuations and promotes a stable coexistence.

Furthermore, for the positive fixed point $E^* = (x^*, y^*)$ of system (1.3), we obtain the following:

$$\frac{\mathrm{d}x^*}{dr} = -\frac{\gamma\eta\sigma\tau}{\beta(\eta\tau - r\sigma + \sigma)^2}, \qquad \frac{\mathrm{d}y^*}{dr} = 0.$$

Since $\frac{\mathrm{d}x^*}{\mathrm{d}r} < 0$, an increase in r results in a decrease in the equilibrium density of the commensal species. This is because the effective interacting fraction $(1 - r)y$ is decreased, thus reducing the gain to the commensal population.

On the other hand, the expression $\frac{\mathrm{d}y^*}{\mathrm{d}r} = 0$ indicates that the host equilibrium is not affected by any changes in r, since it is only governed by intrinsic growth and self-limitation. This further points to the asymmetric nature of the commensal relationship, where the commensal is affected by the host but the converse is not true.

The parameter r serves a dual function in that it not only reduces the equilibrium level of the commensal population but also stabilizes the system by eliminating the complex behavior. This is an

important result in understanding the role of inefficient interactions in controlling population levels in natural systems.

4.4. Two-parameter analysis

In order to obtain a deeper understanding of the global dynamics of system (1.3), we carry out a two-parameter bifurcation analysis where we vary both the step size h and the interaction efficiency parameter r. This allows us to investigate the combined effects of discretization and interaction strength on the system's dynamics.

Keeping $\alpha = 1.8, \beta = 1.1, \gamma = 0.9, \eta = 0.7, \sigma = 0.6$, and $\tau = 1.4$ fixed, with initial conditions $x_0 = 1.8$ and $y_0 = 0.4$, we vary the parameters $h \in [0.8, 1.5]$ and $r \in [0.3, 0.7]$. For each pair (h, r), the system is iterated for 6000 time steps, and the last 2500 iterates are used for the classification of the long-term behavior. A period-p orbit is identified when the mean absolute difference between two consecutive blocks of p asymptotic iterates is less than 10^{-4}. The periods $p = 1, 2, \ldots, 12, 16, 32$, and 64 are examined, where $p = 1$ represents convergence to a fixed point. The classification is further supported by the MLE, with positive values indicating chaotic dynamics. The two-dimensional bifurcation graph in (h, r)-plane is illustrated in Figure 7(a), where distinct colors distinguish various dynamical behaviors such as stable equilibria, periodic solutions of different periods, and chaotic dynamics. The associated MLE is depicted in Figure 7(b), where negative values correspond to either a stable or periodic behavior, while positive values indicate the presence of chaos.

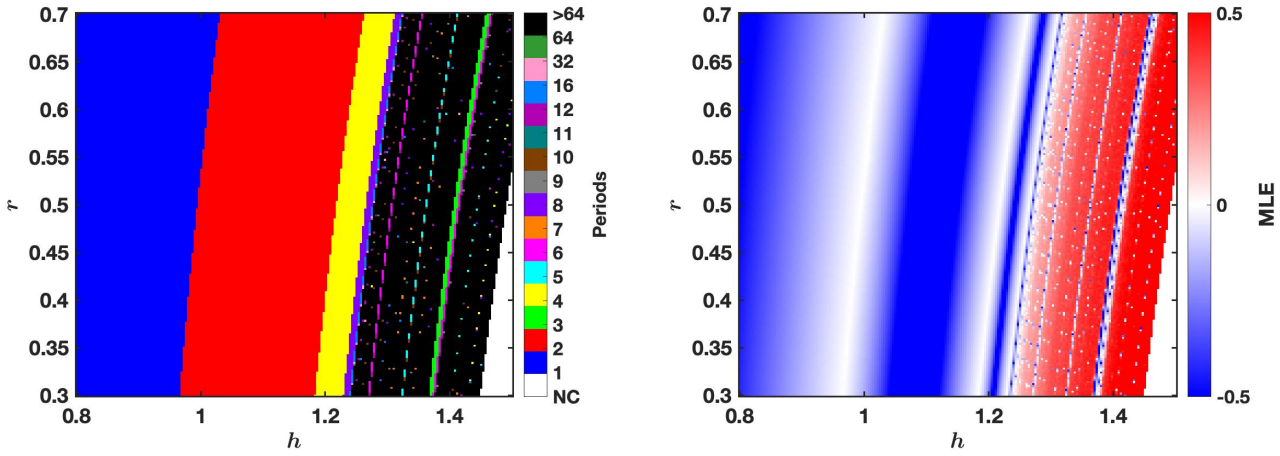

(a) Bifurcation diagram **(b)** MLE plot

Figure 7. Two-dimensional bifurcation diagram and MLE plot of (1.3) varying $h \in [0.8, 1.5]$ and $r \in [0.3, 0.7]$. Fixed values are $\alpha = 1.8, \beta = 1.1, \gamma = 0.9, \eta = 0.7, \sigma = 0.6$, and $\tau = 1.4$, and the initial values are $x_0 = 1.8, y_0 = 0.4$.

The results clearly indicate a strong interaction between h and r. When h takes relatively smaller values, the system remains stable for a very large range of r. However, when h takes larger values, complex dynamics such as a period-doubling bifurcation and chaos are observed for smaller values of r, while larger values of r stabilize the dynamics.

From an ecological standpoint, this analysis illustrates the role of discrete-time effects and the

interaction efficiency. Although large values of h increase the instability by large discrete updates, large values of r actually reduce the interaction and thus stabilize the system. This illustrates how an inefficient interaction can actually help to stabilize a system against large fluctuations and chaos in the commensal species.

5. Conclusions

In this work, a new discrete-time model of commensalism, including saturation effects and the efficiency of interaction, were proposed and examined. The discrete model was obtained from the continuous system using the forward Euler method, which provides a simple and computationally efficient discretization framework. The introduction of the efficiency parameter, which takes the part of the host species that does not interact effectively into account, allows for a more realistic description of the ecological interaction, where not all individuals of a species can equally contribute to the well-being of the commensal species. This is a distinguishing feature of the proposed model compared to many classical commensalism models.

The existence and stability of all possible fixed points were discussed. A detailed analysis of bifurcation was performed, and it was found that the system exhibits a period-doubling bifurcation if the step size parameter varies around critical values. With the help of the center manifold theory and a normal form analysis, it was shown that a stable two-period cycle emerges from the coexistence equilibrium.

The numerical simulations were consistent with the analytical results. Bifurcation diagrams and te time-series behavior clearly showed the dynamics from stable equilibrium to periodic oscillations and chaos, confirming the analytical results. In addition, the basin of attraction analysis revealed the coexistence of multiple attractors for the same set of parameter values, demonstrating the presence of multistability in the proposed system. The intricate basin structures further indicated a strong sensitivity to initial conditions, where small changes in the initial population densities may lead to qualitatively different long-term dynamical behaviors. Moreover, a sensitivity analysis was used to show the relative importance of different parameters, where intraspecific competition and interaction efficiency play an important role in the level of populations, while saturation and host parameters affect long-term dynamics. The two-parameter analysis further showed that the combined variation of h and r strongly influences the dynamical regime: Larger values of h promote periodic and chaotic behaviors, whereas increasing r generally has a stabilizing effect.

In comparison to the currently available commensalism models in the literature, the proposed commensalism model provides a better and more flexible framework by taking the saturation and partial interaction efficiencies into account at the same time. Additionally, the proposed commensalism model provides ecological realism and tractability, unlike the classical models with unbounded interaction terms. Moreover, the discrete-time nature of the proposed commensalism model allows it to have richer dynamics in comparison to the continuous-time commensalism models, including period-doubling and complex oscillations.

Use of Generative-AI tools declaration

The author declares that he has not used Artificial Intelligence (AI) tools in the creation of this article.

Acknowledgments

This study is supported via funding from Prince Sattam bin Abdulaziz University, project number (PSAU/2026/R/1448).

Conflict of interest

The author has no conflicts of interest to disclose.

References

1. X. Liu, D. Xiao, Complex dynamic behaviors of a discrete-time predator-prey system, *Chaos Soliton. Fract.*, **32** (2007), 80–94. https://doi.org/10.1016/j.chaos.2005.10.081
2. C. Mondal, R. Mondal, D. Kesh, D. Mukherjee, Dynamics of predator-prey system with the consequences of double Allee effect in prey population, *J. Biol. Phys.*, **51** (2025), 5. https://doi.org/10.1007/s10867-025-09670-0
3. X. Yu, Z. Zhu, Z. Li, Stability and bifurcation analysis of two-species competitive model with Michaelis-Menten type harvesting in the first species, *Adv. Differ. Equ.*, **2020** (2020), 397. https://doi.org/10.1186/s13662-020-02817-4
4. Y. Yang, L. Ma, B. Duan, R. Zou, Global dynamics of two-species reaction-diffusion competition model with Gompertz growth, *Appl. Anal.*, **103** (2024), 2791–2807. https://doi.org/10.1080/00036811.2024.2319225
5. S. He, X. Hu, Dynamical analysis of a discrete Amensalism system with Beddington-DeAngelis functional response and double Allee effects, *Int. J. Bifurcat. Chaos*, **36** (2026), 2650050. https://doi.org/10.1142/S0218127426500501
6. X. Hu, H. Li, F. Chen, Bifurcation analysis of a discrete Amensalism model, *Int. J. Bifurcat. Chaos*, **34** (2024), 2450020. https://doi.org/10.1142/s0218127424500202
7. S. Jawad, S. K. Hassan, Bifurcation analysis of commensalism intraction and harvisting on food chain model, *Braz. J. Biometrics*, **41** (2023), 218–233. https://doi.org/10.28951/bjb.v41i3.609
8. A. Tassaddiq, R. Ahmed, A. Ditta, Exploring stability and bifurcation in a discretized commensalism model, *Nonlinear Dynam.*, **113** (2025), 28463–28475. https://doi.org/10.1007/s11071-025-11530-4
9. M. B. Almatrafi, Stability and period-doubling bifurcation of fractional-order commensal symbiosis model with Allee effect, *Fractal Fract.*, **10** (2026), 226. https://doi.org/10.3390/fractalfract10040226

10. J. Zhang, Q. Yue, Dynamical behavior of a host-commensal system with multiplicative Allee effect and nonselective harvesting, *Electron. Res. Arch.*, **34** (2026), 6404–6431. https://doi.org/10.3934/era.2026280

11. J. Chen, R. Wu, A Commensal symbiosis model with non-monotonic functional response, *Commun. Math. Biol. Neu.*, **2017** (2017), 5. https://doi.org/10.28919/cmbn/2839

12. T. Li, Q. Wang, Stability and Hopf bifurcation analysis for a two-species Commensalism system with delay, *Qual. Theor. Dyn. Syst.*, **20** (2021), 83. https://doi.org/10.1007/s12346-021-00524-3

13. X. He, Z. Zhu, J. Chen, F. Chen, Dynamical analysis of a Lotka Volterra Commensalism model with additive Allee effect, *Open Math.*, **20** (2022), 646–665. https://doi.org/10.1515/math-2022-0055

14. M. Qu, Dynamical analysis of a Beddington-DeAngelis Commensalism system with two time delays, *J. Appl. Math. Comput.*, **69** (2023), 4111–4134. https://doi.org/10.1007/s12190-023-01913-4

15. J. Zhong, L. Chen, F. Chen, Stability and bifurcation in a two-patch commensal symbiosis model with nonlinear dispersal and additive Allee effect, *Int. J. Biomath.*, **19** (2026), 2450099. https://doi.org/10.1142/s1793524524500992

16. R. R. Patra, S. Maitra, Dynamics of stability, bifurcation and control for a commensal symbiosis model, *Int. J. Dynam. Control*, **12** (2024), 2369–2384. https://doi.org/10.1007/s40435-023-01367-3

17. Y. Chong, A. J. Kashyap, S. Chen, F. Chen, Dynamics analysis of a discrete-time commensalism model with additive Allee for the host species, *Axioms*, **12** (2023), 1031. https://doi.org/10.3390/axioms12111031

18. Q. Din, Stability, bifurcation analysis and chaos control for a predator-prey system, *J. Vib. Control*, **25** (2019), 612–626. https://doi.org/10.1177/1077546318790871

19. Y. Liu, L. Guo, X. Liu, Multiple bifurcation analysis in a discrete-time predator-prey model with Holling IV response function, *Symmetry*, **17** (2025), 1459. https://doi.org/10.3390/sym17091459

20. S. H. Strogatz, *Nonlinear dynamics and chaos: With applications to physics, biology, chemistry, and engineering*, 2 Eds, CRC Press, 2015. https://doi.org/10.1201/9780429492563

21. P. A. Naik, Y. Javaid, R. Ahmed, Z. Eskandari, A. H. Ganie, Stability and bifurcation analysis of a population dynamic model with Allee effect via piecewise constant argument method, *J. Appl. Math. Comput.*, **70** (2024), 4189–4218. https://doi.org/10.1007/s12190-024-02119-y

22. P. A. Naik, R. Ahmed, A. Faizan, Theoretical and numerical bifurcation analysis of a discrete predator-prey system of Ricker type with weak Allee effect, *Qual. Theor. Dyn. Syst.*, **23** (2024), 260. https://doi.org/10.1007/s12346-024-01124-7

23. M. M. Abou Hasan, A. M. Alghanmi, H. Al Ali, Z. Mukandavire, Improved numerical schemes to solve general fractional diabetes models, *Alex. Eng. J.*, **109** (2024), 29–40. https://doi.org/10.1016/j.aej.2024.08.095

24. M. M. Abou Hasan, Variable order fractional diabetes models: Numerical treatment, *Int. J. Model. Simul.*, **46** (2026), 737–751. https://doi.org/10.1080/02286203.2024.2349508

25. A. Suleman, A. Q. Khan, R. Ahmed, Bifurcation analysis of a discrete Leslie-Gower predator-prey model with slow-fast effect on predator, *Math. Method. Appl. Sci.*, **47** (2024), 8561–8580. https://doi.org/10.1002/mma.10032

26. F. Gumusboga, F. Kangalgil, Dynamics of a discrete predator-prey model with an Allee effect in prey: Stability, bifurcation analysis and chaos control, *Int. J. Bifurcat. Chaos*, **35** (2025), 2550097. https://doi.org/10.1142/s021812742550097x

27. S. M. Salman, A. M. Yousef, A. A. Elsadany, Stability, bifurcation analysis and chaos control of a discrete predator-prey system with square root functional response, *Chaos Soliton. Fract.*, **93** (2016), 20–31. https://doi.org/10.1016/j.chaos.2016.09.020

28. A. A. Elsadany, A. M. Yousef, S. A. Ghazwani, A. S. Zaki, Bifurcation analysis of a discrete Basener-Ross population model: Exploring multiple scenarios, *Computation*, **13** (2025), 11. https://doi.org/10.3390/computation13010011

29. J. Guckenheimer, P. Holmes, *Nonlinear oscillations, dynamical systems, and bifurcations of vector fields*, New York: Springer, **42** (1983). https://doi.org/10.1007/978-1-4612-1140-2

30. S. Wiggins, M. Golubitsky, *Introduction to applied nonlinear dynamical systems and chaos*, Springer-Verlag, 2003. https://doi.org/10.1007/b97481

31. Y. A. Kuznetsov, *Elements of applied bifurcation theory*, New York: Springer, 2004. https://doi.org/10.1007/978-1-4757-3978-7

Appendix

A. Nonlinear term coefficients in system (3.2)*:*

$$a_1 = \frac{2\beta(\sigma - r\sigma + \eta\tau)}{(-1+r)\alpha\sigma + (-1+r)\gamma\sigma - \alpha\eta\tau},\ a_2 = \frac{2(-1+r)^2\gamma\eta\tau^3}{\beta((-1+r)\sigma - \eta\tau)^3},$$

$$a_3 = -\frac{2(-1+r)\gamma\eta\tau^2}{((-1+r)\sigma - \eta\tau)((-1+r)\alpha\sigma + (-1+r)\gamma\sigma - \alpha\eta\tau)},\ a_4 = \frac{-((-1+r)\gamma\sigma) + \alpha(\sigma - r\sigma + \eta\tau)}{(-1+r)\sigma - \eta\tau},$$

$$a_5 = -\frac{(-1+r)\gamma\eta\tau^2((-1+r)\alpha\sigma + (-1+r)\gamma\sigma - \alpha\eta\tau)}{\beta((-1+r)\sigma - \eta\tau)^3},\ a_6 = -\frac{2(-1+r)^3\gamma\eta\tau^4}{\beta(\sigma - r\sigma + \eta\tau)^4},\ a_7 = -\beta,$$

$$a_8 = \frac{2(-1+r)^2\gamma\eta\tau^3}{((-1+r)\sigma - \eta\tau)^2((-1+r)\alpha\sigma + (-1+r)\gamma\sigma - \alpha\eta\tau)},$$

$$a_9 = \frac{(-1+r)^2\gamma\eta\tau^3((-1+r)\alpha\sigma + (-1+r)\gamma\sigma - \alpha\eta\tau)}{\beta(\sigma - r\sigma + \eta\tau)^4},$$

$$a_{10} = -\frac{(-1+r)\gamma\eta\tau^2}{(\sigma - r\sigma + \eta\tau)^2},\ b_1 = -\frac{2\tau(\sigma - r\sigma + \eta\tau)}{-((-1+r)\gamma\sigma) + \alpha(\sigma - r\sigma + \eta\tau)},\ b_2 = -\sigma,\ b_3 = -\tau.$$

B. Coefficients associated with the nonlinear terms of system (3.4)*:*

$$c_1 = \frac{2\beta(\sigma - r\sigma + \eta\tau)}{(-1+r)\alpha\sigma + (-1+r)\gamma\sigma - \alpha\eta\tau},$$

$$c_2 = \Big((2(-1+r)\gamma\eta\tau^3((-1+r)\alpha^2((-1+r)\sigma - \eta\tau)^2 - \alpha((-1+r)\sigma - \eta\tau)(-2(-1+r)^2\gamma\sigma + 3(-1+r)^2\sigma^2 - 4(-1+r)\eta\sigma\tau + \eta^2\tau^2) + \sigma((-1+r)^3\gamma^2\sigma - 3(-1+r)^2\gamma\sigma((-1+r)\sigma - \eta\tau) + (2(-1+r)\sigma - \eta\tau)(\sigma - r\sigma + \eta\tau)^2))\Big)\Big/\Big(\beta((-1+r)\sigma - \eta\tau)^3(\sigma(\gamma - r\gamma + (-1+r)\sigma - \eta\tau) + \alpha(\sigma - r\sigma + \eta\tau))^2)\Big),$$

$$c_3 = -\Big(2(-1+r)\gamma\eta\tau^2(\alpha((-1+r)\sigma - \eta\tau) + \sigma((-1+r)\gamma + (-1+r)\sigma - \eta\tau))\Big)\Big/\Big(((-1+r)\sigma - \eta\tau)((-1+r)\alpha\sigma + (-1+r)\gamma\sigma - \alpha\eta\tau)(\sigma(\gamma - r\gamma + (-1+r)\sigma - \eta\tau) + \alpha(\sigma - r\sigma + \eta\tau))\Big),$$

$$c_4 = \frac{-((-1+r)\gamma\sigma) + \alpha(\sigma - r\sigma + \eta\tau)}{(-1+r)\sigma - \eta\tau},$$

$$c_5 = \frac{2(-1+r)^3\gamma\eta\tau^4((-1+r)\alpha\sigma + (-1+r)\gamma\sigma - \alpha\eta\tau + \gamma\eta\tau + \sigma(\sigma - r\sigma + \eta\tau))}{\beta(\sigma - r\sigma + \eta\tau)^4(\sigma(\gamma - r\gamma + (-1+r)\sigma - \eta\tau) + \alpha(\sigma - r\sigma + \eta\tau))},\ c_6 = -\beta,$$

$$c_7 = \frac{2(-1+r)^2\gamma\eta\tau^3}{((-1+r)\sigma - \eta\tau)^2((-1+r)\alpha\sigma + (-1+r)\gamma\sigma - \alpha\eta\tau)},$$

$$c_8 = \frac{1}{\beta(\sigma - r\sigma + \eta\tau)^4}(-1+r)\gamma\eta\tau^3((-1+r)\alpha\sigma + (-1+r)\gamma\sigma - \alpha\eta\tau)\Big(-1+r + \frac{((-1+r)\sigma - \eta\tau)^2}{\sigma(\gamma - r\gamma + (-1+r)\sigma - \eta\tau) + \alpha(\sigma - r\sigma + \eta\tau)} - \frac{(-1+r)\gamma\eta\tau((-1+r)\alpha\sigma + (-1+r)\gamma\sigma - \alpha\eta\tau)}{(\alpha((-1+r)\sigma - \eta\tau) + \sigma((-1+r)\gamma + \sigma - r\sigma + \eta\tau))^2} + \frac{(-1+r)\gamma\eta\tau}{\alpha((-1+r)\sigma - \eta\tau) + \sigma((-1+r)\gamma + \sigma - r\sigma + \eta\tau)}\Big),$$

$$c_9 = -\frac{(-1+r)\gamma\eta\tau^2(\alpha((-1+r)\sigma - \eta\tau) + \sigma((-1+r)\gamma + (-1+r)\sigma - \eta\tau))}{((-1+r)\sigma - \eta\tau)^2(\sigma(\gamma - r\gamma + (-1+r)\sigma - \eta\tau) + \alpha(\sigma - r\sigma + \eta\tau))},$$

$$d_1 = -\frac{2\tau(\sigma - r\sigma + \eta\tau)}{-((-1+r)\gamma\sigma) + \alpha(\sigma - r\sigma + \eta\tau)},\ d_2 = -\sigma,\ d_3 = -\tau.$$